International Journal of Fluid Power 5 (2004) No. 2 pp. 57-66

EFFECT OF CONTROLLER IN REDUCING STEADY-STATE ERROR DUE TO FLOW AND FORCE DISTURBANCES IN THE ELECTROHYDRAULIC ACTUATOR SYSTEM

Eric Sampson, Saeid Habibi, Richard Burton and Yuvin Chinniah

Department of Mechanical Engineering, University of Saskatchewan, 57 Campus Drive, Saskatoon, Saskatchewan, Canada S7N 5A9
eric.s@usask.ca, saeid_habibi@engr.usask.ca, richard_burton@engr.usask.ca, yac494@mail.usask.ca

Abstract

This paper pertains to the nonlinear control of a high-precision hydrostatic actuation system known as the Electro-Hydraulic Actuator (EHA). It describes the action of the controller in reducing the steady state error resulting from flow and force disturbances. The EHA uses inner-loop pump velocity feedback to achieve an unprecedented level of accuracy for a hydrostatic system. A published mathematical model of the EHA is reviewed and expanded to produce an equation that predicts the response of the EHA to both desired inputs as well as flow and force disturbances. This equation suggests that the use of a proportional outer-loop controller should result in steady-state error as a result of these disturbances, but that a PI outer-loop controller should eliminate the steady-state error. Experimental results from a prototype of the EHA demonstrate that due to the nonlinear friction present in the actuator, the use of a conventional proportional or PI controller is not sufficient to effectively deal with these disturbances. However, a nonlinear proportional outer-loop controller does result in a substantial performance improvement in regards to disturbance rejection for positional accuracy. Experiments conducted on the prototype using the nonlinear controller reveal that it is capable of a positional accuracy of 1 μm for a load of 20 kg.

Keywords: actuator, electrohydraulic, hydrostatic, micro-precision, disturbance rejection

1 Introduction

Traditional hydraulic systems have several drawbacks with regards to their use in high-performance applications. These include:

- High energy usage due to the pumps being driven continuously by constant-speed motors even when the actuator is not moving,
- requirement of a large central fluid distribution system including a reservoir, and
- requirement of expensive servo valves for precision control.

A novel hydraulic actuation system referred to as the Electro-Hydraulic Actuator (EHA) has been developed to overcome these drawbacks while providing high positional accuracy, as presented by Habibi and Goldenberg (1999). The EHA uses a bi-directional fixed-displacement pump powered by a variable-speed servomotor, Watton (1989), Arnautovic (1993), Desai and Bobrow (1989), Manring and Lueke (1989), Merrit (1967). The actuator is directly connected to the pump as shown in Fig. 1. The pump¥s speed and direction determine the flow to and from the actuator and hence its displacement. An integral contributor to the high performance of the EHA is inner-loop velocity control of the pump velocity. This reduces the dead-band common in hydrostatic actuation systems that limit their performance and positional accuracy. A prototype of the EHA has demonstrated an excellent level of performance with a nonlinear control approach, being capable of moving a 20 kg load with an accuracy of 1 μm and a critically damped rise time of 0.3 s.

In sections 1 to 6 of the paper, a method is developed to theoretically predict the steady-state positional error of the EHA as a result of both flow and force disturbances. A flow disturbance can be defined as any load flow that is not included in the EHA model, such as changes in actuator seal performance causing additional external leakage. A force disturbance can similarly be defined as any external force applied to the load that is not included in the EHA model. Examples of force disturbances could be nonlinear friction between the rails and the load, or sudden application of an external force.

This manuscript was received on 13 October 2003 and was accepted after revision for publication on 05 July 2004

The development of a way to model these disturbances is important because it allows one the opportunity to simulate the effects of arbitrary time-varying flow and force disturbances on the EHA system using a simulation package on a computer. For this paper, the purpose of developing an EHA model that includes these disturbances was to predict the steady-state error as a result of flow and force disturbances when using a proportional versus a proportional-integral (PI) controller. In section 7 of the paper, experiments that were conducted to verify the accuracy of the predictions are presented; in addition a controller is developed to minimize the steady-state error of the EHA.

2 EHA System

The EHA system consists of the following components:

- Controller
- Electric Motor
- Bi-Directional Gear Pump
- Accumulator
- Pressure, Position and Speed Sensors
- Crossover Relief Valve
- Symmetrical Actuator
- Load

A simplified schematic of the system is shown as Fig. 1.

The three-phase brushless AC electric motor directly drives the pump, which controls the flow of hydraulic oil to the two active chambers of the actuator. Depending on the load, the resulting pressure differential between the actuator chambers then applies a net force on the external load. In this case, the load is a 20 kg steel block mounted on two linear rails which is displaced horizontally by the force exerted on it by the actuator.

The symmetrical linear actuator used in the prototype has a single rod and has been designed expressly for the system, as described in Habibi and Goldenberg (1999). The actuator has two working chambers C1 and C2, illustrated in Fig. 2. The rod is hollow and has a circular disc at the end of the rod inside the actuator. Hydraulic fluid enters the two chambers of the actuator through ports O1and O2.

The working areas of the chambers A1 and A2 are made equal in area, which results in symmetrical flow if leakage is neglected. There also exists a third working chamber C3, which can be pressurized via port O5 to provide a bias to counteract a constant external force. Finally, ports O3 and O4 are provided to drain any actuator fluid leakage.

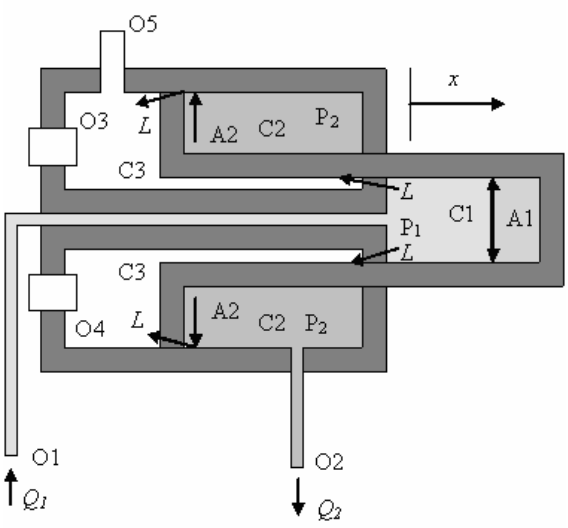

Fig. 2: *Cross-section of actuator*

An accumulator is connected to the low-pressure case drain of the gear pump. It prevents cavitation, and replaces fluid lost due to leakage. The accumulator sets the minimum system pressure and can be adjusted from 0.28-0.69 MPa (40-100 psi). The upper limit is set by the pump seals, which would be damaged if the case drain pressure exceeds 0.69 MPa.

The crossover relief valves increase the safety of the system by preventing excessive pressure build-up if the actuator reaches the end of its travel, or if a fault were to occur. Recently a new position sensor has been added to the system to measure the displacement of the load. The sensor, an optical linear encoder, has a resolution of 1 μm. This sensor has enabled more exact positional data to be obtained, increasing the accuracy of the system.

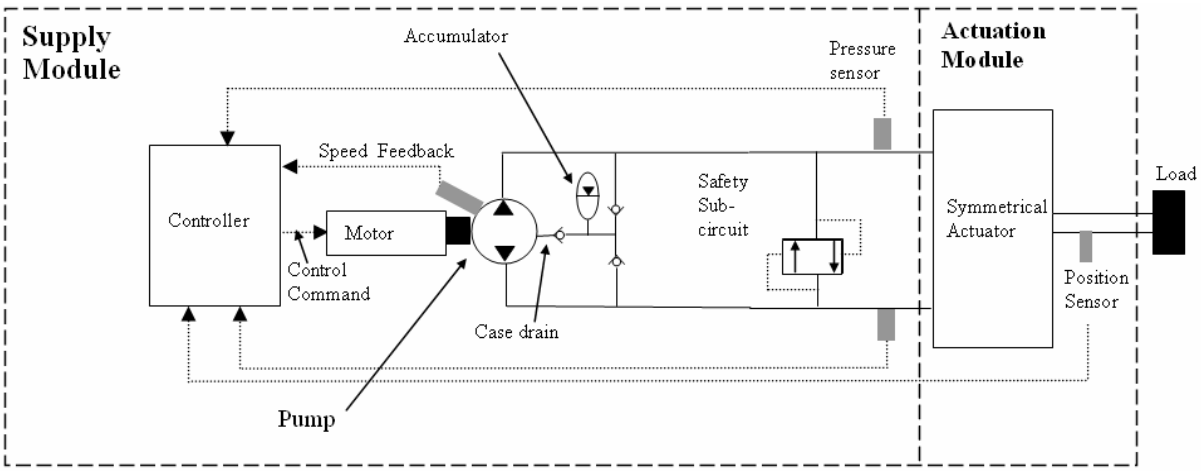

Fig. 1: *Schematic of EHA*

3 EHA Model

A mathematical model of the EHA system was developed in Habibi and Singh (2000). In this paper, an analysis of the effect of flow disturbances and force disturbances on the system is considered by using an expanded EHA model. Figure 3 shows a simplified block diagram for the system showing the outer-loop position controller $G_{OL}(s)$, the inner-loop pump velocity loop $G_V(s)$, and the hydraulic transfer function $G_H(s)$.

The EHA system as described in Habibi and Singh (2000) used a proportional outer-loop controller such that:

$$G_{OL}(s) = \frac{U(s)}{E(s)} = 585 \tag{1}$$

The motor/pump subsystem consists of a bi-directional pump driven directly by an AC electrical motor controlled by a velocity controller. An identified model of the overall motor/pump subsystem transfer function was described in Habibi, Pastrakuljic and Goldenberg (2000). As such, the motor/pump subsystem with a PI inner-loop controller can be described by Eq. 2, an identified transfer function:

$$G_V(s) = \frac{\omega_p(s)}{U(s)} = \frac{0.2779s + 40.55}{5.780\times10^{-5}s^2 + 1.016\times10^{-2}s + 1} \tag{2}$$

Let $\kappa_v = 40.55$, the motor gain.

Further to the hydraulic model of the EHA as described in Habibi and Singh (2000) and neglecting the pressure drop across the lines while introducing a disturbance flow Q_{dis}, a simplified linear relationship is obtained as:

$$D_p\omega_p + Q_{dis} = A\dot{x} + \frac{V_o}{2\beta_e}\left(\frac{dP_1}{dt} - \frac{dP_2}{dt}\right) + \xi(P_1 - P_2) + \frac{L}{2}(P_1 - P_2) \tag{3}$$

From Eq. 3, the resulting transfer function between the actuator pressure differential and the fluid flow is obtained as:

$$\frac{P_1(s) - P_2(s)}{D_p\omega_p(s) + Q_{dis}(s) - AX(s)s} = \frac{1}{\frac{V_o s}{2\beta_e} + \xi + \frac{L}{2}} \tag{4}$$

The EHA prototype has a load that consists of a mass M that slides on horizontal rails that contribute a viscous damping term B, and experiences a disturbance force F_{dis}. This results in the following load model:

$$(P_1 - P_2)A + F_{dis} = M\ddot{x} + B\dot{x} \text{ or} \tag{5}$$

$$\frac{X(s)s}{(P_1(s) - P_2(s))A + F_{dis}(s)} = \frac{1}{Ms + B} \tag{6}$$

Combining Eq. 1, 2, 4 and 6 results in the system block diagram shown in Fig. 4. Included in dashed lines in Fig. 4 is the hydraulic transfer function $G_H(s)$, which relates the output $X(s)$ to the input flow $D_p\omega_p(s) + Q_{dis}(s)$.

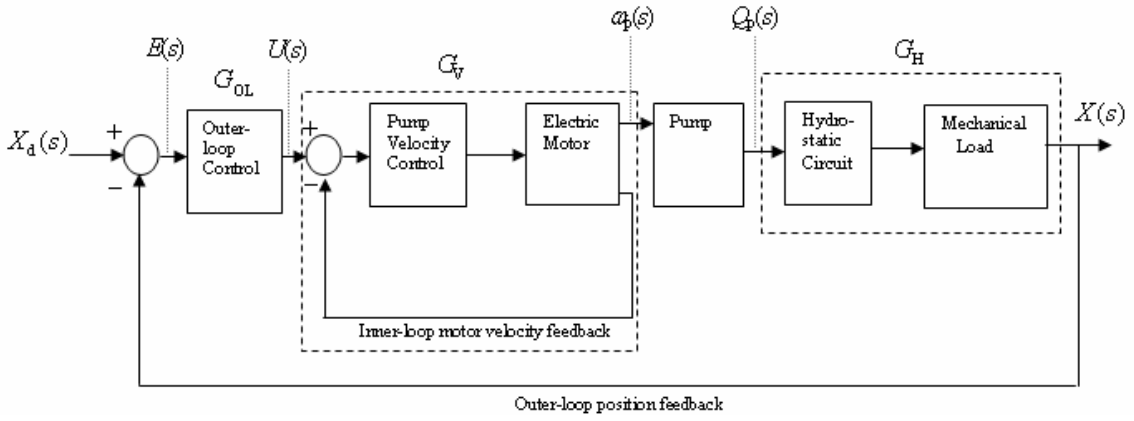

Fig. 3: *Simplified EHA block diagram*

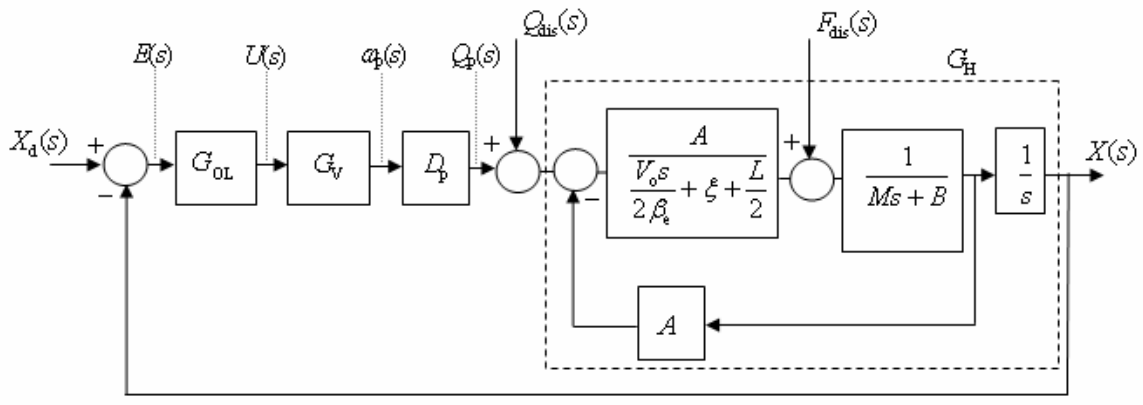

Fig. 4: *EHA block diagram showing hydraulic transfer function $G_H(s)$*

4 Effect of Flow Disturbances

The inclusion of a term for flow disturbances, $Q_{dis}(s)$, in the EHA model allows for the investigation of external pump leakage and other sources of flow disturbance, including changes in actuator seal performance. It will now be shown that the EHA system using a proportional controller will theoretically exhibit a steady-state error if there is a constant flow disturbance $Q_{dis}(s)$.

In order to demonstrate this, it is desirable to obtain the transfer function between the flow disturbance $Q_{dis}(s)$ and the output $X(s)$. To do so, the inputs $X_d(s)$ and $F_{dis}(s)$ shown in Fig. 4 are set to zero. Since $F_{dis}(s) = 0$, the hydraulic transfer function $G_H(s)$ shown in dashed lines in Fig. 4 can be expressed in the standard form as:

$$G_H(s) = \frac{X(s)}{D_p\omega_p(s) + Q_{dis}(s)} = \frac{\kappa_h \omega_{nh}^{\ 2}}{s(s^2 + 2\zeta_h\omega_{nh}s + \omega_{nh}^{\ 2})} \tag{7}$$

where

$$\kappa_h = \frac{2A}{2A^2 + (2\xi + L)B}$$

$$\zeta_h = \left(\frac{B}{2M\omega_{nh}} + \frac{(2\xi + L)\beta_e}{2V_o\omega_{nh}}\right) \text{ and}$$

$$\omega_{nh} = \sqrt{\left(\frac{2\beta_e A^2 + (2\xi + L)\beta_e B}{MV_o}\right)}$$

Rearranging Fig. 4 allows the relationship between the flow disturbance $Q_{dis}(s)$ and the output $X(s)$ to be illustrated in a conventional manner, as shown in Fig. 5.

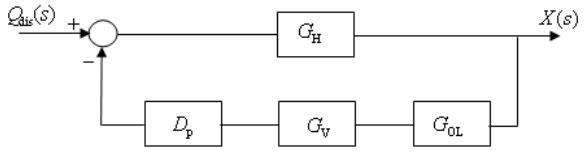

Fig. 5: *Block diagram for flow disturbances*

From Fig. 5, the transfer function between $Q_{dis}(s)$ and $X(s)$ can be derived as:

$$\frac{X(s)}{Q_{dis}(s)} = \frac{G_H(s)}{1 + G_H(s)D_pG_V(s)G_{OL}(s)} \tag{8}$$

or

$$\frac{X(s)}{Q_{dis}(s)} = \frac{\kappa_h \omega_{nh}^{\ 2}}{\left[\begin{array}{l}\{s(s^2 + 2\zeta_h\omega_{nh}s + \omega_{nh}^{\ 2})\ldots \\ \quad + \kappa_h\omega_{nh}^{\ 2}D_pG_V(s)G_{OL}(s)\}\end{array}\right]} \tag{9}$$

To investigate the effect of flow disturbances on the position of the actuator, the final value theorem is used to determine the steady-state error E_{ss} in the system output, given a step flow disturbance $Q_{dis}(s) = 1\times10^{-7}/s$ m^3/s. This disturbance flow was selected because it is approximately 10% of the maximum pump flow that occurs when the system is moved 0.01 m in 1 sec.

$$E_{ss} = \lim_{s\to0}\left[sQ_{dis}(s)\frac{X(s)}{Q_{dis}(s)}\right] = \left[\frac{sQ_{dis}(s)}{D_p\kappa_vG_{OL}(s)}\right]_{s\to0} \tag{10}$$

It should be noted that even though the model of the hydraulic system is Type 1 (as indicated by Eq. 7), the steady-state error is not alleviated in the presence of flow disturbances. This can be intuitively verified by considering the integral action of the hydraulic transfer function. Since the integral action is downstream of the error source, as shown in Fig. 4, the system will integrate the error causing the actuator to move. This will continue until the error becomes of the same magnitude as the flow disturbance but of opposite sign. When that occurs, the input of the integrator becomes zero since the integrated error signal and the flow disturbance will cancel each other out. The result is that the output position will then remain fixed at a non-zero steady-state error.

Since the steady-state error predicted by Eq. 10 includes the transfer function of the outer-loop controller $G_{OL}(s)$, the response of the EHA to flow disturbances depends on the type of controller adopted. This is now considered.

4.1 Proportional Controller

The initial design of the EHA system as presented by Habibi and Singh (2000) employed a proportional outer-loop controller with $G_{OL}(s) = K_p = 585$. Using this controller, Eq. 10 predicts the steady-state error as a result of a 1×10^{-7} m^3/s step flow disturbance to be:

$$E_{ss} = \left[\frac{1\times10^{-7}}{6.863\times10^{-6}(585)}\right]_{s\to0} = 24.9\mu\text{m} \tag{11}$$

This analysis indicates that a step flow disturbance of 1×10^{-7}m^3/s would theoretically result in a steady-state position error of 25 μm. This implies that, when using a proportional controller with the EHA, significant actuator displacements may occur as a result of flow disturbances that are less than ten percent of the pump flow $Q_P(s)$.

4.2 Proportional-Integral Controller

The steady-state error in response to a step flow disturbance is theoretically eliminated if an integrator is introduced upstream of the location where the disturbance enters the system model. This can be achieved if the outer-loop controller is changed from proportional to proportional-integral,where

$G_{OL}(s) = K_p + \frac{K_i}{s} = 585 + \frac{K_i}{s}$ such that:

$$E_{ss} = \left[\frac{1\times10^{-7}}{6.863\times10^{-6}\left(585+\frac{K_i}{s}\right)} \right]_{s\to 0} = 0\text{m} \qquad (12)$$

This suggests that adding integral action to the outer-loop controller before the disturbance input theoretically eliminates the steady-state position error as a result of the flow disturbance. However, as will be shown in the experimental data, the practical aspect of using integral action to reduce steady state error at the micrometer level is not without its problems.

Specifically, the presence of nonlinear friction in the actuator results in limit cycle oscillation. Due to the small magnitude of the error present near steady state, it takes a significant amount of time for the integrator to accumulate enough control action in order to overcome the static friction of the motionless actuator. When it does, the actuator will accelerate rapidly since the dynamic friction is smaller in magnitude than the static friction, resulting in an overshoot of the desired position. The instantaneous error then drives the error accumulated in the integrator towards zero thus holding the actuator at a position with non-zero steady-state error. The entire cycle will then repeat, resulting in the limit cycle oscillation seen in Fig. 12.

5 Effect of Force Disturbances

The effect of force disturbances on the actuator may be modelled in a similar manner to the flow disturbances discussed above. If the inputs $X_d(s)$ and $Q_{dis}(s)$ are set to zero, the relationship between $X(s)$ and $F_{dis}(s)$ may be illustrated by rearranging the system block diagram of Fig. 4 to produce Fig. 6.

From Fig. 6 the transfer function between $X(s)$ and $F_{dis}(s)$ may be determined by simplifying the block diagram to obtain the following:

$$\frac{X(s)}{F_{dis}(s)} = \frac{1/M}{s^2 + \frac{B}{M}s + \frac{\kappa_h \omega_{nh}{}^2 (As + D_p G_V(s) G_{OL}(s))}{s + (2\xi + L)\beta_e / V_o}} \qquad (13)$$

The final value theorem can be used as in Eq. 14 to determine the actuator system output when the input is a step force disturbance $F_{dis}(s) = 1000/s$ N. This value of force disturbance was selected as it represents the force applied by gravity to a vertical actuator by a nominal human mass of 100 kg. This situation could occur if a person were to sit down on a positioning table controlled in the vertical axis by an EHA.

$$\begin{aligned} E_{ss} &= \lim_{s\to 0}\left[sF_{dis}(s)\frac{X(s)}{F_{dis}(s)} \right] \\ &= \left[\frac{sF_{dis}(s)(2\xi + L)}{2AD_p\kappa_v G_{OL}(s)} \right]_{s\to 0} \end{aligned} \qquad (14)$$

Equation 14 implies that the response of the EHA to force disturbances depends on the type of outer-loop controller adopted, similar to the response of the EHA to flow disturbances. This dependency is now considered.

5.1 Proportional Controller

Using Eq. 14, the response to a 1000 N force disturbance can be predicted for the original proportional outer-loop controller $G_{OL}(s) = K_p = 585$ as:

$$E_{ss} = \left[\frac{1000}{22950(585)} \right]_{s\to 0} = 74\mu\text{m} \qquad (15)$$

This analysis indicates that a force disturbance of 1000 N would theoretically result in a significant steady-state positional error of 74 μm.

5.2 Proportional-Integral Controller

The steady-state error in response to a step force disturbance is theoretically eliminated if the outer-loop controller is changed from proportional to proportional-integral, where $G_{OL}(s) = K_p + \frac{K_i}{s} = 585 + \frac{K_i}{s}$ such that:

$$E_{ss} = \left[\frac{1000}{22950\left(585+\frac{K_i}{s}\right)} \right]_{s\to 0} = 0\text{m} \qquad (16)$$

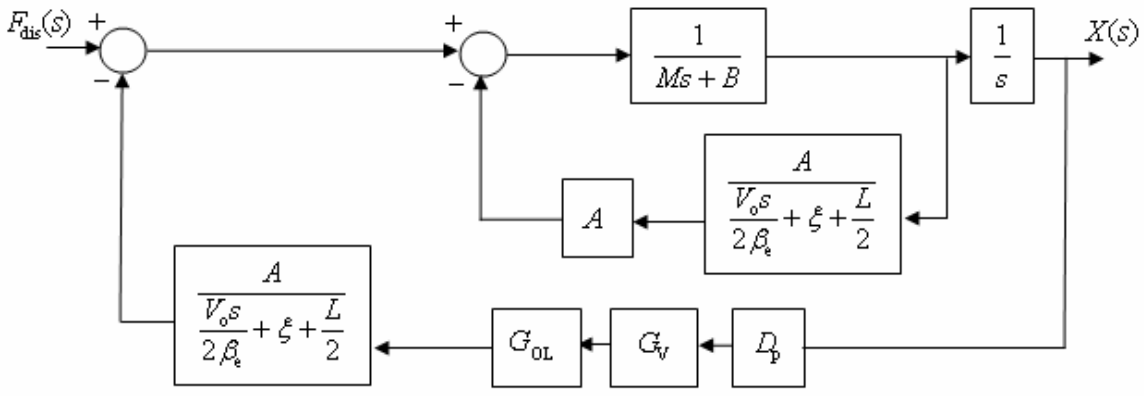

Fig. 6: *Block diagram for force disturbances*

6 Complete EHA Transfer Function

From the block diagram in Fig. 4 and setting the disturbance inputs $Q_{dis}(s)$ and $F_{dis}(s)$ to be zero, a transfer function may be determined between the actuator position $X(s)$ and the desired position $X_d(s)$:

$$\frac{X(s)}{X_d(s)} = \frac{\kappa_h \omega_{nh}^2 D_p G_V(s) G_{OL}(s)}{\left[\begin{array}{l}\{s(s^2 + 2\zeta_h \omega_{nh} s + \omega_{nh}^2)\ldots \\ \quad + \kappa_h \omega_{nh}^2 D_p G_V(s) G_{OL}(s)\}\end{array}\right]} \quad (17)$$

Substituting the relevant parameters with $G_{OL}(s) = K_p = 585$ into Eq. 17 in MATLAB® Simulink produced the theoretical closed-loop response to a 10 mm step input shown in Fig. 7.

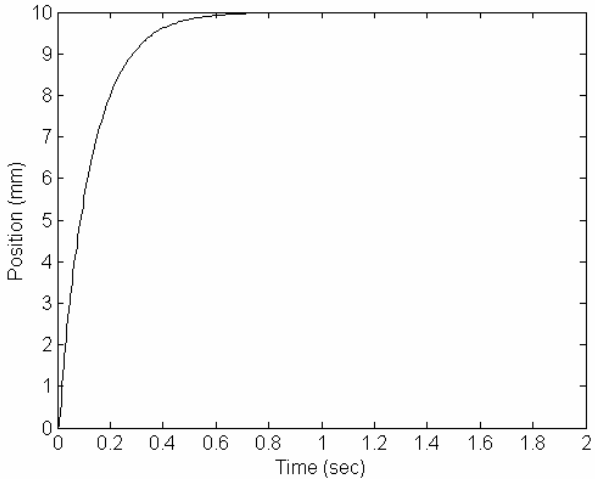

Fig. 7: *Theoretical response to 10 mm step input*

Using the principal of superposition for a linear system, Eq. 9, 13 and 17 can be combined to produce Eq. 18. This equation predicts the output $X(s)$ of the EHA given any combination of the three time-varying inputs: desired position $X_d(s)$, flow disturbance $Q_{dis}(s)$, and force disturbance $F_{dis}(s)$.

$$X(s) = \frac{X(s)}{X_d(s)} X_d(s) + \frac{X(s)}{Q_{dis}(s)} Q_{dis}(s) \ldots + \frac{X(s)}{F_{dis}(s)} F_{dis}(s) \quad (18)$$

Equation 18 is useful because it allows the response of the system to arbitrary disturbances to be simulated that would be complicated using mathematical analysis. For instance, one could predict the system response if the load was travelling with constant velocity and the actuator experienced additional load resistance as a result of increased friction due to local damage to the load rails. This could be accomplished by setting the desired position input $X_d(s)$ to be a linearly increasing function, and then adding a step friction force to the force disturbance input $F_{dis}(s)$. Similarly, one could predict the effect of a change in external actuator leakage while the actuator is maintaining a constant position. This could be modelled by applying the desired position signal to the input $X_d(s)$, and then adding a small negative flow to the flow disturbance input $Q_{dis}(s)$ after the actuator position has settled.

In summary, the theoretical analysis presented here leads to an equation that can be used for predicting the response of the EHA with respect to the desired input as well as arbitrary time-varying flow and force disturbances. This equation demonstrates that constant flow and force disturbances will result in steady-state positional errors if a proportional outer-loop controller is used. However, a proportional-integral controller theoretically eliminates steady-state error as a result of these disturbances. Experimental results however prove otherwise due to the nonlinear effects that are only dynamically significant when dealing with extreme positional accuracy in this system as discussed in the following section.

7 Effect of Controller on Experimental Performance

In sections 1 to 6, the steady-state error of the EHA as a result of ì noiseî due to flow and force disturbances was predicted. In the following section, these predictions are tested experimentally to verify their accuracy.

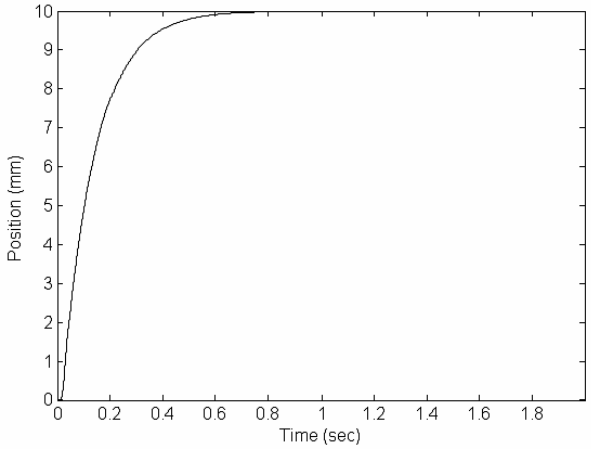

Fig. 8: *Experimental response to 10 mm step input*

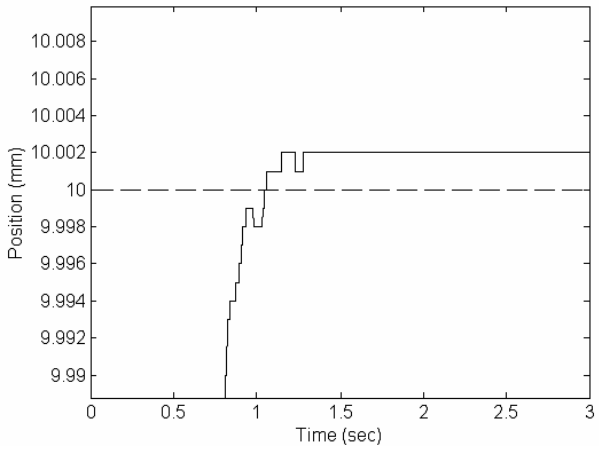

Fig. 9: *Response to step input near steady state for proportional controller*

Figure 8 shows the experimental system response to a 10 mm step input with the EHA connected to a 20 kg horizontally-sliding load. This response is obtained using the proportional controller $G_{OL}(s) = K_p = 585$ as employed in Habibi and Singh (2000). From this graph the 0.3 s rise time and the 0.6 s settling time of the system can be observed. Figure 9 shows a magnified ver-

sion of Fig. 8, demonstrating the steady-state error of 2 μm as theoretically predicted in Habibi and Goldenberg (2000). The position sensor employed is an optical encoder with 0.17 m travel, 1 μm resolution and an accuracy of ±3 μm/m. The sampling time for all the experiments was 0.001 s.

7.1 Gain Scheduling

Since the overall time response of the system with the original proportional controller was excellent, it was desirable to maintain this overall response while reducing the steady-state error of 2 μm. Gain scheduling is a method that can be used to provide two control strategies in order to achieve this goal. When the error signal is large, the original proportional controller is employed. However, when the error signal becomes small as the actuator approaches the steady-state position, an additional control element is added. Because the error signal is very small at the time that the additional controller is added, its gain can be very high without causing saturation of the system or excessive overshoot.

Due to the fact that gain scheduling is employed for the nonlinear integral and nonlinear proportional controllers, the overall system response as shown in Fig. 8 will not change appreciably. However, the response near their steady-state accuracy level, as shown in Fig. 9 with the proportional controller, will vary.

7.2 Nonlinear Integral Controller

As predicted by Eq. 12 and 16, an integral outer-loop controller would theoretically eliminate the steady-state error present in Fig. 9. However, experience and simulations indicated that adding simple integral action to the existing controller would increase the percentage overshoot significantly. This was not acceptable, as it was desired to maintain the overall system response as shown in Fig. 8.

In order to add integral action to the controller without affecting the large-signal response, a nonlinear outer-loop integral controller as shown in Fig. 10 was employed. This sets the input of the integrator to zero when the error signal is more than ±5 μm, and switches on the integrator when the error is less than 5 μm. This error threshold was chosen because it is slightly larger than the typical steady-state error of 2-3 μm.

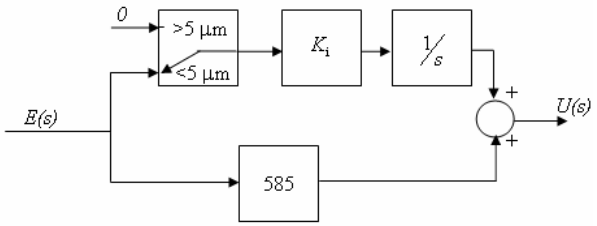

Fig. 10: *Nonlinear outer-loop integral controller*

Step input tests with a magnitude of 10 mm were performed using the nonlinear integral controller with K_i = 0, 500, 1000 and 1500. The results are shown below in Fig. 11, which has been magnified to show detail. Until approximately 3 seconds, the response of the system is similar regardless of the integral gain K_i. After this time, the response differs depending on the integral gain employed.

It can be seen that with a low integral gain of K_i = 500, the steady-state error is reduced to less than 1 μm. However, the 3.5 seconds required to achieve this state is unacceptably long. Higher integral gains reduced the amount of time required for the system to overcome static friction, but resulted in limit cycle oscillation. This is due to the nonlinear friction present in the actuator, which causes the actuator to overshoot the desired position, stick and repeat as shown in Fig. 12.

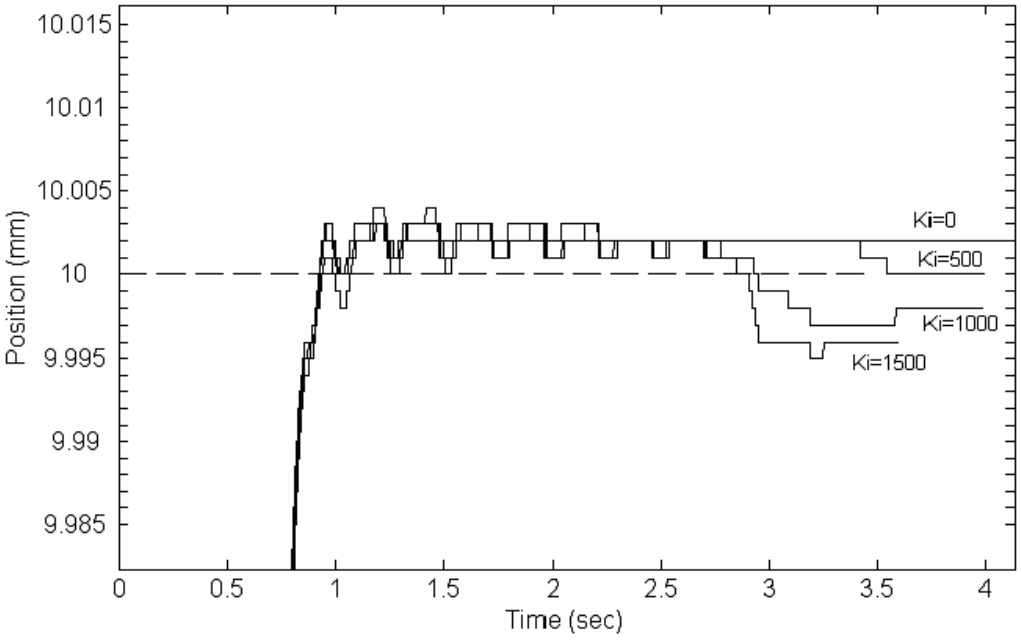

Fig. 11: *Experimental step response with varying integral gains*

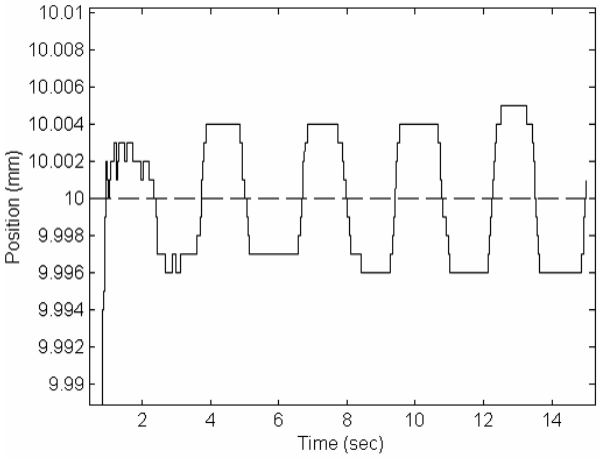

Fig. 12: *Experimental step response with integral gain K_i = 500*

For this reason, nonlinear integral control was found to be an ineffective method of reducing steady-state error in the EHA system. Nonlinear proportional control was the next approach to be examined.

7.3 Nonlinear Proportional Controller

A gain and phase margin analysis of the EHA model with a proportional controller was performed using MATLAB®. The original system with controller $G_{OL}(s) = K_p = 585$ has 26 dB of gain margin and 88 degrees of phase margin. It was found that K_p could be increased to 3585 while maintaining an acceptable 10 dB of gain margin and 76 degrees of phase margin, Ogata (2002).

This gain level was chosen because it was experimentally determined to be effective in decreasing the steady-state error to less than the resolution of the position sensor. To avoid altering the original response of the system, the proportional gain was split up into two parts; a fixed gain of 585 and a switched gain of 3000 that was added when the error signal was less than the ±5 μm error threshold that was discussed earlier. This nonlinear proportional controller can be seen in Fig. 13.

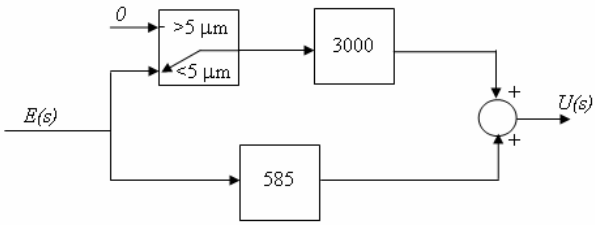

Fig. 13: *Nonlinear outer-loop proportional controller*

This nonlinear proportional control strategy of greatly increasing the stiffness of the controller when the position error becomes small was very effective with the EHA. Figure 14 shows a magnified graph of the response of the system to a 10 mm step input. It can be seen that the error becomes less than the 1 μm resolution of the optical encoder in approximately 1.5 seconds.

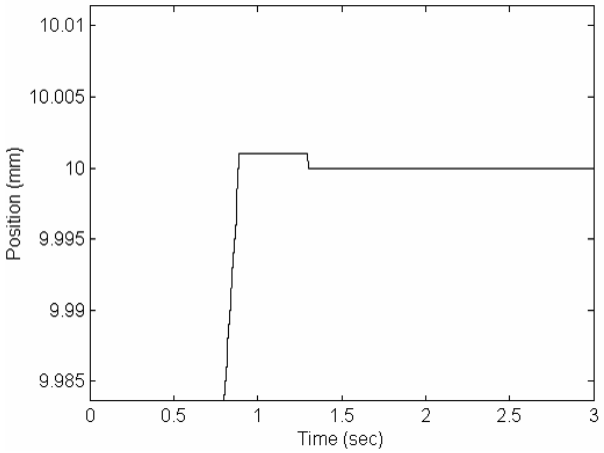

Fig. 14: *Experimental step response with nonlinear proportional controller*

The same control strategy also enables repeatable steps as small as 1 μm to be performed, as shown in Fig. 15 in response to a 1 μm step input. The output of the position sensor is discrete with a 1 μm resolution ±0.5 quantum. Therefore, the response shown in the Fig. 15 indicates only that the steady-state position is within ±0.5 μm of the desired position and does not show the details of the actuator¥s movement.

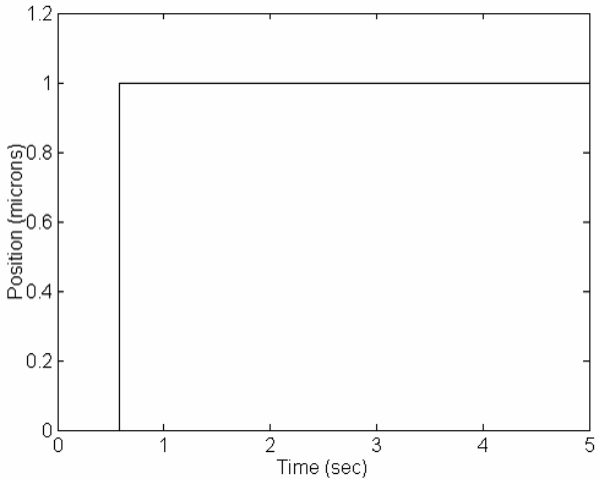

Fig. 15: *Experimental 1 μm step response*

Finally, a test was conducted to verify the nonlinear proportional controller¥s ability to reject force disturbances while maintaining a constant position. The desired input $X_d(s)$ was set to be zero, and the load was struck moderately with a hammer in the axial direction three times. The impulse generated by the hammer was calculated to be approximately 40 N from knowledge of the active area of the actuator and the differential pressure across it during the impulse. This test was intended to simulate impulsive force disturbances, such as a mass being dropped onto a positioning table controlled in the vertical axis by an EHA.

Figure 16 shows the experimental response to the impulse force disturbances. It can be seen that the EHA returns to its original position, within 1 μm, in approximately 1 second. This demonstrates that the nonlinear proportional controller is indeed capable of

rejecting force disturbances while maintaining the desired transient response and providing 1 μm positional accuracy.

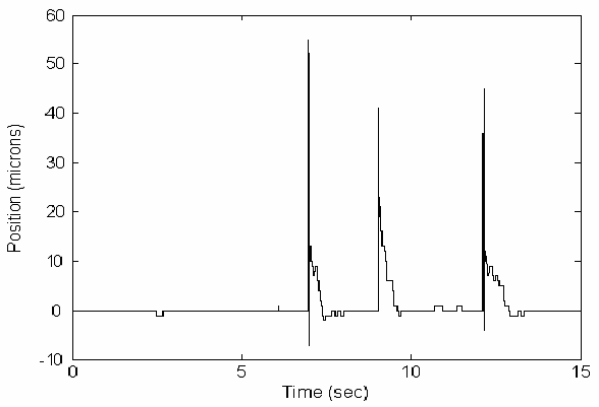

Fig. 16: *Experimental force impulse rejection response*

8 Conclusions

The Electro-Hydraulic Actuator (EHA) model presented in Habibi and Singh (2000) has been expanded to include inputs for flow and force disturbances, producing a single equation that predicts the response of the EHA to both desired inputs and disturbance inputs. An analysis using this equation suggests that using the proportional outer-loop controller will result in steady-state error with constant force and flow disturbances. It also suggests that a proportional-integral outer-loop controller will eliminate the steady-state error as a result of the disturbances.

Tests were conducted to verify these predictions. Nonlinear controllers were used in an effort to retain the desirable overall response of the proportional controller while reducing its 2 μm steady-state error. The nonlinear integral controller was found to be ineffective, as low integral gains took too long to reduce the steady-state error and higher integral gains resulted in limit cycle oscillation as a result of nonlinear load friction. In contrast, a nonlinear proportional outer-loop control strategy reduced the steady-state error as a result of these disturbances to the limit of the optical encoder accuracy. Furthermore, this control strategy demonstrated the ability to reject force impulse disturbances, returning to the desired position within 1 μm while preserving the systemís transient response and positional accuracy.

Using the nonlinear proportional controller, the EHA demonstrated a high level of performance. With a 20 kg load, the encoder positional accuracy of 1 μm was achieved while preserving critical damping and very satisfactory settling and rise times. Repeatable steps of 1 μm were exhibited despite the presence of nonlinear friction in the system.

With this level of performance, the EHA has applications in areas requiring precise positioning unprecedented in conventional fluid power and geared electrical actuation systems. Furthermore, the EHA is compact, modular, energy efficient, and capable of a high force output.

Nomenclature

$A1 = A2 = A$	Actuator pressure area	5.05×10^{-4} m^2
B	Coefficient of friction at load	*760 N/m/s
$C1, C2, C3$	Actuator chambers	
D_p	Pump volumetric displacement	1.6925×10^{-7} m^3/rad
$E(s)$	Error signal	V
E_{ss}	Steady-state positional error	m
$F_{dis}(s)$	External force displacement	N
$G_{OL}(s)$	Outer loop controller	
$G_V(s)$	Motor/Pump subsystem transfer function	
$G_H(s)$	Hydraulic transfer function	
K_p, K_i	Controller gains	
L	Leakage coefficient	$*2\times 10^{-15}$ m^3/s/Pa
M	Load mass	20 kg
$O1, O2, O3, O4, O5$	Actuator ports	
P_1, P_2	Actuator chamber pressure	Pa
Q_1, Q_2	Actuator chamber flow	m^3/s
$Q_{dis}(s)$	Disturbance flow	m^3/s
$Q_p(s)$	Pump flow	m^3/s
$U(s)$	Motor input voltage	V
V_o	Pipe plus mean actuator chamber volumes	6.1×10^{-5} m^3
$X(s)$	Position of actuator	m
$X_d(s)$	Demanded position of actuator	m
β_e	Effective bulk modulus of hydraulic oil	$*2.1\times 10^{8}$ Pa
κ_h	Hydraulic gain	
κ_v	Motor gain	40.55 rad/s/V
ω_{nh}	Hydraulic undamped natural frequency	
$\omega_p(s)$	Pump angular velocity	rad/s
ξ	Pump cross-port leakage coefficient	$*1.5\times 10^{-13}$ m^3/s/Pa
ζ_h	Hydraulic damping ratio	

* values obtained from Chinniah (2004)

References

Arnautovic, S. 1993. *Electrohydraulic Actuator*. Technical Report, University of Toronto, Canada.

Chinniah, Y. 2004. *Fault Detection in the Electrohydraulic Actuator Using Extended Kalman Filter*. Phd thesis, University of Saskatchewan, Canada.

Desai, J. and **Bobrow, J**. 1989. Modelling and Analysis of a High Torque Hydrostatic Actuator for Robotic Applications. *Exp. Robotics*.

Habibi, S. and **Goldenberg, A**. 1999. Design and Analysis of a Symmetrical Linear Actuator for Hydraulic Systems. *Transactions of the CSME*, Vol. 23, No. 3 & 4, pp. 377-397.

Habibi, S. and **Goldenburg, A.** 2000. Design of a New High Performance Electrohydraulic Actuator. *IEEE/ASME Transactions on Mechatronics,* Vol. 5, No. 2.

Habibi, S., Pastrakuljic, V. and **Goldenburg, A.** 2000. Model Identification and Analysis of a High Performance Hydrostatic Actuation System. *SAE paper 2000-01-2619, 2000 SAE International Off-Highway & Powerplant Congress and Exposition*.

Habibi, S. and **Singh, G.** 2000. Derivation of Design Requirements for Optimization of a High Performance Hydrostatic Actuation System. *International Journal of Fluid Power,* Vol. 1, No. 2.

Manring, N. and **Lueke, G**. 1998. Modelling and Designing a Hydrostatic Transmission with a Fixed-Displacement Motor. *Journal of Dyn. Sys. Meas. & Cont,* Vol. 120, pp. 45-50.

Merritt, H. 1967. *Hydraulic Control Systems*. John Wiley & Sons.

Ogata, K. 2002. *Modern Control Engineering, 4th Ed*. Prentice Hall.

Watton, J. 1989. *Fluid Power Systems.* Prentice Hall.

Eric Sampson
Received his B.Sc. in Mechanical Engineering in 2003 from the University of Saskatchewan, Canada. Performed research in the Department of Mechanical Engineering during the summer of 2003 as a NSERC USRA recipient. He is currently pursuing his M. Sc. at the same University in the area of intelligent control. His research interests include advanced control systems, robotics and MEMS.

Saeid Habibi
Obtained his Ph.D. in Control Engineering and Robotics from the University of Cambridge, UK. He worked as a project manager and senior consultant for Cambridge Control Ltd, UK and as manager of Systems Engineering for Allied Signal Aerospace Canada. His academic background includes research into design and analysis of hydraulic actuation systems, sensors and instrumentation and advanced multivariable control. He is on the Editorial Board of the CSME and a member of IEEE. He is currently an Associate Professor in Mechanical Engineering at the University of Saskatchewan, Canada.

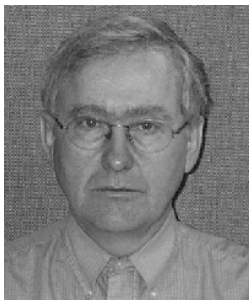

Richard Burton
P.Eng, Ph.D, Assistant Dean, Professor, Mechanical Engineering, University of Saskatchewan. Burton is involved in research pertaining to the application of intelligent theories to control and monitoring of hydraulics systems, component design, and system analysis. He is a member of the executive of ASME, FPST Division, a member of the hydraulics' advisory board of SAE and NCFP and one of members of the international editorial board for FPNI.

Yuvin Chinniah
Ph.D. Candidate in the Mechanical Engineering Department, University of Saskatchewan, Canada. He was the recipient of a Canadian Commonwealth Scholarship in 1999. He obtained his B.Eng. (Hons), First Class, in Electrical and Electronic Engineering in Mauritius (1997). He also worked as an electrical engineer at Dynamotors Ltd in Mauritius for two years. His research interest includes fluid power control, control systems and estimation techniques such as the Kalman Filter.